

RESEARCH PAPER

## X-Ray Diffraction and Electron Microscopy in the Polymorphism Study of Ondansetron Hydrochloride

J. M. Liácer,<sup>1</sup> V. Gallardo,<sup>1</sup> R. Delgado,<sup>2</sup>  
J. Párraga,<sup>2</sup> D. Martín,<sup>3</sup> and M. A. Ruiz<sup>1,\*</sup>

<sup>1</sup>Department of Pharmacy and Pharmaceutical Technology,

<sup>2</sup>Department of Edaphology and Agricultural Chemistry, and

<sup>3</sup>Department of Mineralogy and Petrology, University of Granada,  
E-18071, Granada, Spain

### ABSTRACT

*Using different techniques, we studied the possible formation of ondansetron polymorphs. Ondansetron is a carbazol antiemetic that acts as a competitive, selective inhibitor of 5-HT<sub>3</sub> serotonin receptors. The polymorphs were determined by X-ray diffraction (XRD) and scanning electron microscopy (SEM). The results suggest that the compounds are not true crystallographic polymorphs, but instead are the product of physical structural changes in the drug, which would be of interest pharmaceutically.*

**Key Words:** Ondansetron hydrochloride; Polymorphs; Scanning electron microscopy; X-ray diffraction

### INTRODUCTION

*Polymorphism* is the ability of any element or compound to crystallize in two or more different forms, giving rise to a structure and properties as

different as the crystals of distinct compounds, thus varying the solubility of the active principles (1,2). The most widely used technique in the investigation of the polymorphism of pharmaceuticals is powder X-ray diffraction (PXRD). The use of PXRD is

\*Corresponding author. M. A. Ruiz, Department of Pharmacy and Pharmaceutical Technology, Faculty of Pharmacy, University of Granada, E-18071 Granada, Spain. Fax: +34-58-248958; E-mail: adolfina@platon.ugr.es

particularly indicated when the routine technique of differential scanning calorimetry (DSC) leads one to suspect the existence of polymorphs (3). PXRD is only used when X-ray quality crystals cannot be obtained, as otherwise X-ray crystallography is employed. In this article, we also examine another procedure that can aid in the analysis of possible polymorphs, scanning electron microscopy (SEM).

The aim of this study was the determination of possible polymorphs of ondansetron hydrochloride, which is a carbazol antiemetic that acts as a competitive, selective inhibitor of 5-HT<sub>3</sub> serotonin receptors (4–6). This mechanism of action makes ondansetron hydrochloride useful in controlling nausea and vomiting induced by cytotoxic chemotherapy and radiotherapy and postoperative vomiting in patients who have undergone gynecological surgery.

## EXPERIMENTAL

Ondansetron hydrochloride 1,2,3,9-tetrahydro-3-[(2-methylimidazole-1-yl)methyl]-9-methyl-4H-carbazol-4-one hydrochloride dihydrate (C<sub>18</sub>H<sub>19</sub>N<sub>3</sub>OHCl·2H<sub>2</sub>O) was supplied by Vita S. A. (Barcelona, Spain). Temperature and solvents were used as modifying factors to obtain the ondansetron polymorphs. The effects of temperature were investigated by heating samples to 150°C for 20 min. To test polymorph formation in different solvents, we prepared dispersions in methanol, ethanol, and chloroform (3).

For the PXRD analyses, the samples were finely ground (<65 µm) and scanned in a powder X-ray diffractometer (Philips PW 1730 diffractometer, CuK<sub>α</sub>, 35 kV, and 15 mA) set at 65–2° 2θ. The Fisher quartz standard was used for the correct reading of the spacing ( $d_{hkl}$ ).

### X-Ray Crystallography

X-ray quality crystals were prepared by recrystallization from methanol solutions of a mixture of enantiomers (racemate). A translucent crystal with dimensions 0.20 × 0.20 × 0.16 mm was used for the X-ray diffractometry. Ondansetron hydrochloride crystallizes in monoclinic space group P2<sub>1</sub>/n. Unit cell parameters and other crystallographic details are summarized in Table 1.

X-ray data were collected on a Siemens R3m/V four-circle diffractometer using graphite crystal monochromated Mo-K<sub>α</sub> radiation ( $\lambda = 0.71073$ ). Accurate

Table 1

Unit Cell Parameters and Other Crystallographic Details

Crystal size (mm)	0.20 × 0.20 × 0.20
Unit cell dimensions	<b>a</b> = 15.103 (3) Å <b>b</b> = 9.741 (2) Å <b>c</b> = 12.757 (3) Å $\beta$ = 100.83 (3)°
Volume	1843.4 (6) Å <sup>3</sup>
Empirical formula	C <sub>18</sub> H <sub>23</sub> ClN <sub>3</sub> O <sub>3</sub>
Formula weight	364.84
Z	4
Calculated density	1.315 mg/m <sup>3</sup>
Absorption coefficient	0.229 mm <sup>-1</sup>
F000	772

cell parameters were obtained by least-squares fit for 25 reflections measured by  $a + \omega$  and  $-\omega$  scan in the range  $2\theta < 30^\circ$ . For intensity data collection, the following parameters were used: temperature 293 K;  $\omega$  scan mode; learn profile method; minimum and maximum measuring times 0.5 and 2 s, respectively, with a scanning range of 1.00° plus  $K_\alpha$  separation;  $2\theta$  range from 3° to 60°; index ranges  $0 = h = 19$ ,  $-12 = vk = 0$ ,  $-16 = l = 16$ . Data were corrected for Lorentz polarization and absorption effects with the  $\Psi$  data collection method ( $\Psi = 5^\circ$ ). Maximum and minimum transmission factors were 0.9642 and 0.9556.  $R_{\text{int}} = 0.0001$ . All independent data were used in the last refinement from collected/independent 4136/4136.

The structure was solved using Patterson methods (7). Atomic scattering factors used were taken from the program. Full-matrix least-squares refinement of  $F^2$  was used, with anisotropic thermal parameters for all nonhydrogens, giving the residuals [ $I > 2\sigma(I)$ ]  $R1 = 0.0699$ ,  $wR2 = 0.1576$ ; and [all data]  $R1 = 0.1147$ , and  $wR = 0.1961$ . There were 267 parameters that were refined. Goodness of fit was on  $F^2$  0.877. The extinction correction was  $F^* = F[1 + 0.001xF_c^2\lambda^3/\sin(2\theta)]^{-1/4}$ ,  $x = 0.012$  (2). The weighting scheme was  $w^{-1} = \sigma^2(F2) + (0.0596P)^2 + 1.30P$ ,  $P = (F_o^2 + F_c^2)/3$ . All hydrogen atoms were located from difference-Fourier syntheses and then were refined isotropically. The largest difference peaks and holes after the last refinement cycle were 0.691 and  $-0.247e^{-3}$ , respectively.

### Solution and Refinement

The system used was a SHEL97 (DOS) program; we used a Patterson solution. The graphics editor

was the XP Siemens program package and SHELXTL PLUS (MSDOS). Our refinement method was full-matrix least squares of the SHELXL program, and the quantity minimized was  $\Sigma w(F_o^2 - F_c^2)^2$ . All the hydrogen atoms were observed. On the last cycle, prior geometric fixation and a constraint of the hydrogen distances were used. The hydrogen atoms were then isotropically refined together with the rest of the atom structures.

The following constraint codes of the SHELX program were used: AFIX 13 for tertiary CH; AFIX 23 for secondary CH<sub>2</sub>; AFIX 33 for primary CH<sub>3</sub>. Initial distances were fixed at 0.85 for O–H and 0.96 (1)  $\pm$  0.01 for C–H.

Final index descriptions were as follows:

$$R2 = \left[ \sum [w(F_o^2 - F_c^2)^2] / \sum [\omega(F_o^2)] \right]^{1/2}$$

$$R1 = \sum F_o - F_c / \sum F_o$$

$$S = \left[ \sum [w(F_o^2 - F_c^2)^2] / (n - p) \right]^{1/2}$$

$R2$ , the weighted  $R$  factor  $wR2$ , and all goodnesses of fit  $S$  were based on  $F^2$ . Conventional  $R$  factors were based on  $F$ , with  $F$  set to zero for negative  $F^2$ . The observed criterion of  $F^2 > 2\theta(F^2)$  was used only for calculating the  $R$  factor and the like and is not relevant to the choice of reflections for refinement.  $R$  factors based on  $F^2$  are statistically about twice as large as those based on  $F$ , and  $R$  factors based on ALL data are even larger.

Atomic coordinates are given in Table 2, selected bond distances in Table 3, selected bond angles in Table 4, anisotropic thermal parameters in Table 5, hydrogen atom coordinates in Table 6, hydrogen bonds in Table 7, and torsion angles in Table 8. Observed and calculated structure factors are provided as supplementary material.

**Table 2**

*Atomic Coordinates ( $\times 10^4$ ) and Equivalent Isotropic Displacement Parameters ( $\text{\AA}^2 \times 10^3$ )*

	<i>x</i>	<i>y</i>	<i>z</i>	<i>U</i> (eq)
N (1)	3981 (2)	−996 (3)	9576 (2)	42 (1)
C (2)	3513 (2)	127 (3)	9252 (3)	38 (1)
C (21)	3355 (3)	1288 (4)	9948 (3)	55 (1)
N (3)	3233 (2)	21 (3)	8203 (2)	38 (1)
C (4)	3532 (2)	−1202 (4)	7860 (3)	48 (1)
C (5)	3997 (2)	−1845 (4)	8722 (3)	50 (1)
C (6)	2690 (2)	1025 (4)	7496 (3)	44 (1)
C (7)	1747 (2)	520 (4)	7084 (3)	52 (1)
C (8)	1220 (2)	1582 (3)	6330 (3)	39 (1)
O (8)	1608 (2)	2499 (3)	5946 (2)	65 (1)
C (9)	260 (2)	1401 (3)	6098 (2)	31 (1)
C (10)	−429 (2)	2173 (3)	5409 (2)	33 (1)
C (11)	−432 (2)	3324 (3)	4763 (3)	43 (1)
C (12)	−1249 (2)	3825 (4)	4237 (3)	50 (1)
C (13)	−2053 (2)	3208 (4)	4329 (3)	50 (1)
C (14)	−2080 (2)	2060 (4)	4958 (3)	42 (1)
C (15)	−1256 (2)	1561 (3)	5497 (2)	35 (1)
N (16)	−1078 (2)	450 (3)	6197 (2)	39 (1)
C (16)	−1762 (3)	−487 (5)	6447 (3)	62 (1)
C (17)	−168 (2)	373 (3)	6565 (2)	34 (1)
C (18)	298 (2)	−623 (3)	7364 (3)	43 (1)
C (19)	1219 (3)	−42 (5)	7851 (4)	70 (1)
Cl (1)	4136 (1)	734 (1)	13109 (1)	61 (1)
O (1W)	6093 (2)	−64 (5)	14475 (3)	95 (1)
O (2W)	4753 (3)	−1492 (4)	11613 (2)	75 (1)

$U(\text{eq})$  is defined as one-third of the trace of the orthogonalized  $U_{ij}$  tensor.

**Table 3***Bond Lengths (Å) for Ondansetron Hydrochloride*

N (1)–C (2)	1.325 (4)
N (1)–C (5)	1.371 (4)
C (2)–N (3)	1.330 (4)
C (2)–C (21)	1.485 (5)
N (3)–C (4)	1.375 (4)
N (3)–C (6)	1.470 (4)
C (4)–C (5)	1.343 (5)
C (6)–C (7)	1.506 (5)
C (7)–C (19)	1.478 (6)
C (7)–C (8)	1.530 (5)
C (8)–O (8)	1.221 (4)
C (8)–C (9)	1.435 (4)
C (9)–C (17)	1.385 (4)
C (9)–C (10)	1.441 (4)
C (10)–C (11)	1.391 (4)
C (10)–C (15)	1.407 (4)
C (11)–C (12)	1.379 (5)
C (12)–C (13)	1.379 (5)
C (13)–C (14)	1.381 (5)
C (14)–C (15)	1.391 (4)
C (15)–N (16)	1.398 (4)
N (16)–C (17)	1.368 (4)
N (16)–C (18)	1.458 (4)
C (17)–C (18)	1.485 (4)
C (18)–C (19)	1.523 (5)

Scanning electron microscopy (SEM) analysis completed the research (Hitachi S-510, Japan) (8). Samples for SEM examination were coated with gold.

## RESULTS AND DISCUSSION

### Powder X-Ray Diffraction

A representative selection of the PXRD diagrams is presented in Fig. 1. The scanning window is constant from 22° to 38° 2 $\theta$  (approximately between 0.403 nm and 0.279 nm).

The main reflections were examined ( $I/I_0 > 20\%$ ) where the peak was largest and there was the greatest proportion of intense reflections (see Tables 9 and 10).

#### Intensities

With respect to the original ondansetron hydrochloride diagram, the polymorph diagram obtained at 150°C inverted the order of the highest

**Table 4***Bond Angles (°) for Ondansetron Hydrochloride*

C (2)–N (1)–C (5)	109.7 (3)
N (3)–C (2)–N (1)	107.5 (3)
N (3)–C (2)–C (21)	127.2 (3)
N (1)–C (2)–C (21)	125.3 (3)
C (2)–N (3)–C (4)	109.0 (3)
C (2)–N (3)–C (6)	126.9 (3)
C (4)–N (3)–C (6)	124.1 (3)
C (5)–C (4)–N (3)	107.3 (3)
C (4)–C (5)–N (1)	106.5 (3)
N (3)–C (6)–C (7)	112.3 (3)
C (19)–C (7)–C (6)	118.8 (3)
C (19)–C (7)–C (8)	112.7 (3)
C (6)–C (7)–C (8)	110.2 (3)
O (8)–C (8)–C (9)	123.4 (3)
O (8)–C (8)–C (7)	121.0 (3)
C (9)–C (8)–C (7)	115.6 (3)
C (17)–C (9)–C (8)	122.4 (3)
C (17)–C (9)–C (10)	107.3 (3)
C (8)–C (9)–C (10)	130.3 (3)
C (11)–C (10)–C (15)	118.9 (3)
C (11)–C (10)–C (9)	134.7 (3)
C (15)–C (10)–C (9)	106.3 (3)
C (12)–C (11)–C (10)	118.5 (3)
C (13)–C (12)–C (11)	121.7 (3)
C (12)–C (13)–C (14)	121.6 (3)
C (13)–C (14)–C (15)	116.7 (3)
C (14)–C (15)–N (16)	129.3 (3)
C (14)–C (15)–C (10)	122.5 (3)
N (16)–C (15)–C (10)	108.1 (3)
C (17)–N (16)–C (15)	108.8 (2)
C (17)–N (16)–C (18)	126.8 (3)
C (15)–N (16)–C (18)	124.4 (3)
N (16)–C (17)–C (9)	109.5 (3)
N (16)–C (17)–C (18)	125.9 (3)
C (9)–C (17)–C (18)	124.6 (3)
C (17)–C (18)–C (19)	108.4 (3)
C (7)–C (19)–C (18)	115.6 (4)

intensities; thus, the first one was 3.71 (100%), and the second one was 3.84 (78%).

Curiously, in the methanol diagram, the second reflection (95%) was the 3.20 one, which was only 53% in the normal diagram.

A similar circumstance occurred with chloroform, although in this case, the 3.20 reflection was 70%.

The ethanol diagram was very like the normal one, although it very slightly inverted the two most intense reflections.

**Table 5**  
Anisotropic Displacement Parameters ( $\text{\AA}^2 \times 10^3$ )

	$U_{11}$	$U_{22}$	$U_{33}$	$U_{23}$	$U_{13}$	$U_{12}$
N (1)	40 (2)	45 (2)	40 (2)	6 (1)	6 (1)	8 (1)
C (2)	33 (2)	40 (2)	42 (2)	3 (1)	6 (1)	1 (1)
C (21)	66 (3)	47 (2)	54 (2)	−8 (2)	11 (2)	11 (2)
N (3)	31 (1)	43 (2)	40 (1)	1 (1)	2 (1)	6 (1)
C (4)	47 (2)	51 (2)	46 (2)	−6 (2)	6 (2)	12 (2)
C (5)	53 (2)	46 (2)	52 (2)	−3 (2)	13 (2)	16 (2)
C (6)	37 (2)	46 (2)	49 (2)	12 (2)	3 (1)	6 (2)
C (7)	40 (2)	49 (2)	64 (2)	20 (2)	0 (2)	0 (2)
C (8)	36 (2)	40 (2)	41 (2)	8 (1)	5 (1)	−3 (1)
O (8)	39 (1)	69 (2)	86 (2)	40 (2)	6 (1)	−7 (1)
C (9)	34 (2)	28 (1)	32 (1)	2 (1)	7 (1)	0 (1)
C (10)	36 (2)	31 (2)	31 (1)	−6 (1)	6 (1)	2 (1)
C (11)	40 (2)	39 (2)	47 (2)	8 (2)	1 (1)	−1 (1)
C (12)	55 (2)	45 (2)	45 (2)	6 (2)	−1 (2)	9 (2)
C (13)	40 (2)	55 (2)	49 (2)	−9 (2)	−8 (2)	13 (2)
C (14)	31 (2)	49 (2)	45 (2)	−7 (2)	4 (1)	−3 (1)
C (15)	36 (2)	36 (2)	32 (2)	−5 (1)	6 (1)	−1 (1)
N (16)	36 (1)	42 (2)	38 (1)	0 (1)	6 (1)	−9 (1)
C (16)	49 (2)	78 (3)	59 (2)	14 (2)	8 (2)	−29 (2)
C (17)	36 (2)	34 (2)	30 (2)	−1 (1)	5 (1)	−3 (1)
C (18)	45 (2)	40 (2)	45 (2)	9 (2)	8 (1)	−2 (2)
C (19)	45 (2)	82 (3)	77 (3)	48 (3)	0 (2)	−3 (2)
Cl (1)	58 (1)	64 (1)	60 (1)	2 (1)	12 (1)	0 (1)
O (1W)	59 (2)	152 (4)	75 (2)	28 (3)	17 (2)	7 (2)
O (2W)	111 (3)	63 (2)	45 (2)	7 (2)	0 (2)	24 (2)

The anisotropic displacement factor exponent takes the form  $-2\pi^2 [(ha^*)^2 U_{11} + \dots + 2hka^*b^*U_{12}]$ .

### Shapes of the Peaks

The most noteworthy point is the splitting of the peak at 3.71–3.65 and 3.50–3.47 in the methanol diagram, which were one-plateau peaks in the normal diagram, indicating a change in intensity.

Again, a single peak in the normal diagram was split into a double peak (2.96–2.99) in the chloroform diagram. In the other diagrams, the peaks seem to be displaced.

In the ethanol diagram, the 3.71–3.67 plateaued peak changed in shape, becoming sharper and intensifying up to 3.71.

The differences in intensity found in the diffraction diagrams of the distinct crystallizations (methanol, ethanol, and chloroform) in Fig. 1 were not due to the formation of different polymorphs since that would entail changes in the unit cell and consequently of the spacings, which were constant here.

The differences in the intensities can be accounted for simply because the crystalline particles used to obtain the powder diagrams are not strictly randomly oriented. This is one of the main drawbacks of PXRD in the structural study of chemical compounds in general.

The sample heated to 150°C did show some changes in the spacing, although again, this does not mean that a different polymorph was formed. Rather, there was a dilation (the unit cell and, consequently, the spacings are further apart), and some adsorption water may have been lost.

### X-Ray Crystallography

The X-ray diffraction (XRD) crystallography technique was used exclusively for the methanol samples as they were the only ones that gave rise to crystals. As can be seen in Fig. 2 and 3, the

**Table 6**  
*Hydrogen Coordinates ( $\times 10^4$ ) and Isotropic Displacement Parameters ( $\text{\AA}^2 \times 10^3$ ) for Ondansetron Hydrochloride*

	<i>x</i>	<i>y</i>	<i>z</i>	<i>U</i> (eq)
H (1)	4210 (3)	−1170 (4)	10,220 (3)	53 (11)
H (21A)	3634	1091	10,673	130 (2)
H (21B)	2719	1411	9905	93 (16)
H (21C)	3610	2111	9717	120 (2)
H (4)	3430	−1526	7162	40 (9)
H (5)	4276	−2697	8737	78 (14)
H (6A)	2982	1217	6897	83 (14)
H (6B)	2662	1875	7884	99
H (7)	1824	−258	6622	140 (2)
H (11)	105	3745	4687	34 (8)
H (12)	−1259	4599	3808	51 (10)
H (13)	−2590	3574	3958	43 (9)
H (14)	−2621	1642	5018	46 (9)
H (16A)	−2346	−195	6082	160 (3)
H (16B)	−1746	−485	7203	140 (3)
H (16C)	−1644	−1398	6220	490 (11)
H (18A)	367	−1496	7023	62 (12)
H (18B)	−54	−770	7916	72 (13)
H (19A)	1136	681	8347	220 (5)
H (19B)	1570	−762	8260	71 (12)
H (1WA)	5510 (4)	210 (6)	14,060 (4)	110 (2)
H (1WB)	6020 (4)	−230 (6)	15,070 (4)	110 (2)
H (2WA)	5070 (3)	−2160 (5)	11,850 (4)	73 (14)
H (2WB)	4660 (4)	−950 (6)	12,140 (5)	130 (2)

**Table 7**  
*Hydrogen Bonds for Ondansetron Hydrochloride (and Degrees)*

D–H...A	<i>d</i> (D–H)	<i>d</i> (H...A)	<i>d</i> (D...A)	<(DHA)
O (2W)–H (2WB)...Cl (1)	0.89 (5)	2.28 (6)	3.143 (4)	164 (5)
O (1W)–H (1WA)...Cl (1)	0.98 (5)	2.25 (5)	3.231 (4)	177 (5)
O (1W)–H (1WB)...Cl (1) #1	0.81 (5)	2.42 (5)	3.232 (4)	178 (6)
O (2W)–H (2WA)...Cl (1) #2	0.83 (4)	2.37 (4)	3.165 (4)	161 (4)
N (1)–H (1)...O (2W)	0.85 (4)	1.83 (4)	2.685 (4)	177 (4)

Symmetry transformations used to generate equivalent atoms: #1,  $-x + 1, -y, -z + 3$ ; #2,  $-x + 1, y - 1/2, -z + 5/2$ .

determination was good and complete since all the hydrogen atoms were observed. The existence of H1 (linked to N1) is quite clear.

Despite these results, we obtained overly high agreement indices (especially  $R1 = 0.0699$ ) because, in molecules with a similar number of electrons, values close to zero can be found (about  $R1 = 0.02$ ).

**Table 8**  
*Selected Torsion Angles for Ondansetron Hydrochloride ( $^\circ$ )*

C (19)	C (7)	C (6)	N (3)	49.5
C (8)	C (7)	C (6)	N (3)	−178.4
C (4)	N (3)	C (6)	C (7)	70.1
C (2)	C (4)	N (3)	C (6)	−109.8

**Table 9**  
*Intensities of the Angular Section of 22 a 38° 2θ*

Reflex (Å)	Ondansetron	150°C	Methanol	Chloroform	Ethanol
3.84 (3.88)	100	78	100	100	98
3.71 (3.67)	97	100	78	79	100
3.50–3.47	55	53	64	47	55
3.29	20	31	28	29	25
3.20	53	62	95	70	54
2.96 (2.94)	63	59	65	66	63

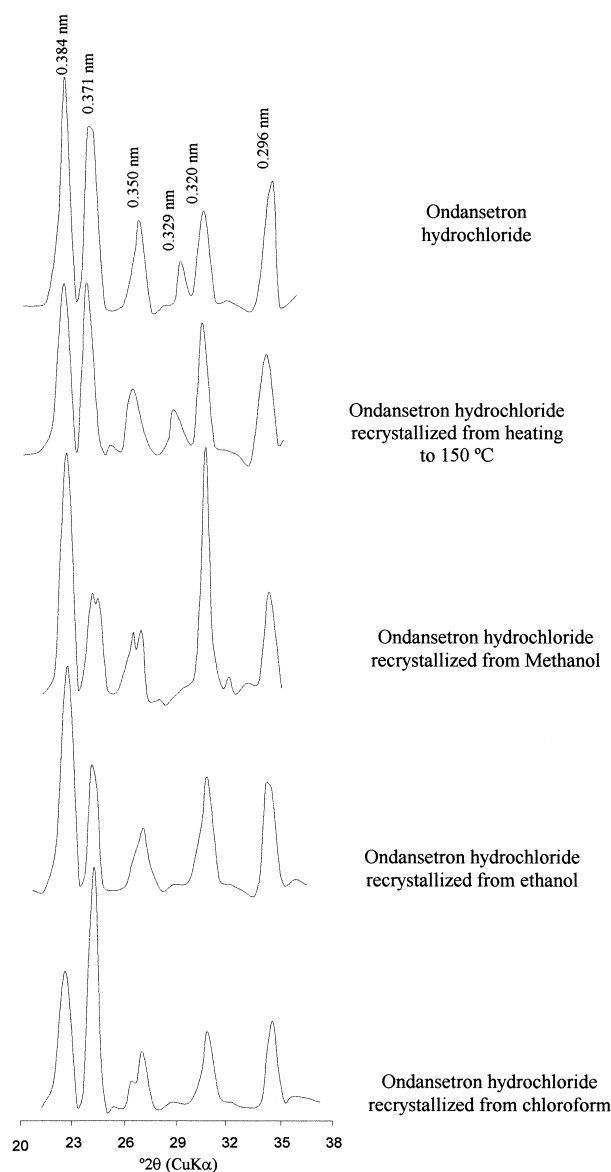


**Figure 1.** Powder X-ray diffraction (PXRD) diagrams for different samples.

These values can be considered very high first by taking into account that the number of electrons of the formula unit ( $F000 = 772$ ) was small. Nevertheless, we showed in the refinement diverse order-disorder defects that impeded good organization of the crystalline structure in short, medium, and long ranges. They limit the minimum value of  $R$  and  $wR$  indices during refinement.

We observed the following structural disorders:

1. The water molecules that coordinate to the chlorine atoms (see Fig. 2) form a very irregular tetrahedron; they present very high thermal factor values. Residual picks of electronic density surroundings to O2W are compatible with an occupational disorder of the position of the hydrogens (H2WA) versus H1.
2. The C7 is a chiral center that is located next to seat position atoms C19, inside the six-ring carbon atoms. We have observed residual picks of electronic density that suggest occasionally inverted positions in diverse parts of the volume crystal (approximately 3% of C7 atoms) and make C19 located in a position near the actual H7 hydrogen atom.
3. There is also thermal disorganization (vibrational disorder due to the temperature) in the hydrogens of the methyl groups. In the case of C16, H16A, H16B, and H16C are found 50% of the time at the sites shown in the diagram and the other 50% of the time at intermediate sites, easily explained by the degree of freedom allowed by the turning of the N16–C16 link. This behavior is also observed in the geometry of the thermal ellipsoid of C16, which is similar in appearance to a flattened ellipsoid. The same can be said of C21.

Water (O1W, O2W) acts as a crystallizing force through hydrogen bonds (see Table 6 for angles,

Type of Peak Sector 22 a 38° 2θ

Reflex ( $\text{\AA}$ )	Ondansetron	150°C	Methanol	Chloroform	Ethanol
3.84 (3.88)	Single peak	Single peak	Single peak	Single peak	Single peak
3.71 (3.67)	Peak (3.71) with plateau (3.67)	Single peak	Double peak	Broad peak	Single peak with small plateau
3.50–3.47	Peak (3.47) with plateau (3.50)	Peak (3.47) with plateau (3.50) with split	Double peak	Single peak with small plateau	Peak (3.47) with plateau (3.50)
3.29	Single peak	Single peak	Single peak	Single peak	Single peak
3.20	Single peak	Single peak	Single peak	Single peak	Single peak
2.96 (2.94)	Single peak	Single peak	Single peak	Double peak (2.96–2.94)	Single peak

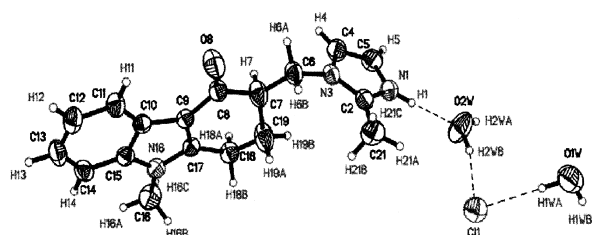


**Figure 2.** X-ray diffraction (XRD) crystallography for crystals of ondansetron hydrochloride with methanol.

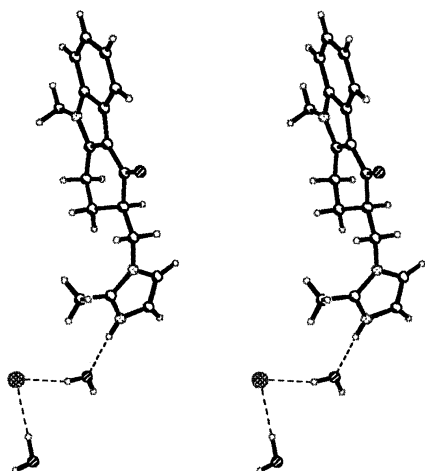


**Figure 3.** Stereo view of the ondansetron hydrochloride molecule.

distances, and standard deviations). These hydrogen bonds, weaker than the intramolecular bonds, explain their very large thermal factors and contribute to the great anisotropic ellipsoid sizes, with the biggest of those observed in the crystalline structure.

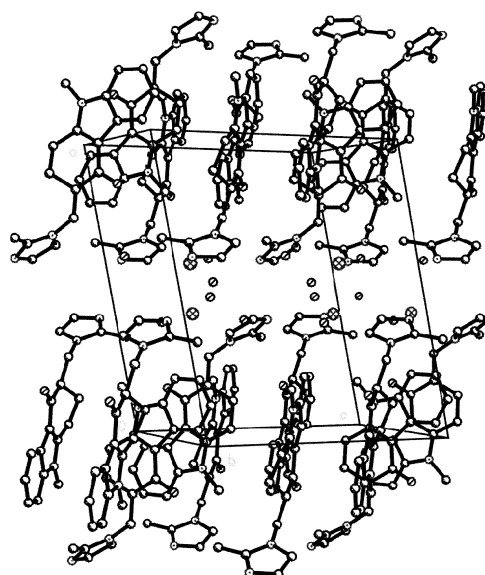


**Figure 4.** Packing diagram and unit cell for crystals of ondansetron hydrochloride with methanol.

Chlorine also acts as a crystallizing force, sandwiched between the enantiomer complex (Fig. 4). Each chlorine molecule is surrounded by four water molecules inside an extremely deformed tetrahedron. Two of the water molecules belong to the same asymmetric unit as described in Table 2. The other two molecules belong to the asymmetric units indicated in Table 7.

The two enantiomers related to each other by the symmetry operation  $[-x, -y, 1-z]$  (symmetry code 2556) demonstrate an absolute parallelism [angle = 0.0(0) degrees] between the two aromatic rings lying between C7 and C19 (Fig. 5a–5c). The distance



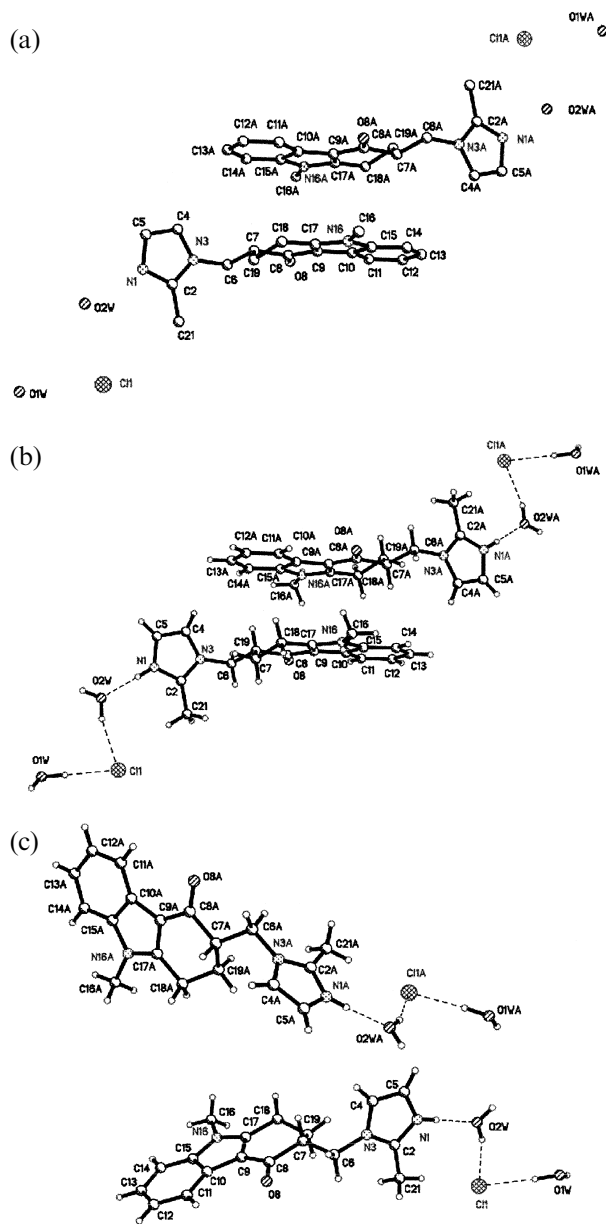


**Figure 5.** (a)–(c) Perspective views for the enantiomers of ondansetron hydrochloride.

between these two planes is between 3.7 and 4 ppm, so the stacking forces between the two enantiomers comprise a crystallizing force (this circumstance in itself nearly entirely justifies the requirement of the 1:1 proportion in this crystal; we note again that the group spacing was central symmetric C21/c). When the mixture of these two enantiomers in the starting active principle were not present in a proportion of 1:1, the crystallization would have the effect of a filter, system-

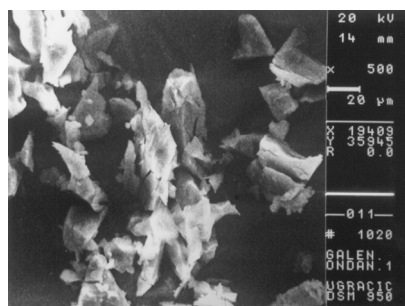


**Figure 6.** Scanning electron microphotographs of ondansetron hydrochloride.

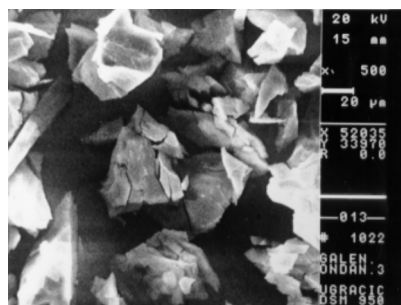


**Figure 7.** Scanning electron microphotographs of ondansetron dissolved in methanol.

atically selecting a molecule of each type and leaving the excess of the more abundant one in the solution or even forming a different crystalline phase (very probably without a symmetrical center). Some of the molecules (very few) would get past the filter and rise to the defect observed here. A good crystallization (very slow, for instance) would produce crystals like the one studied here, but lacking the defects caused by the enantiomery (and therefore in exactly a 1:1 proportion).

### Electron Microscopy

SEM reveals very few differences among the five preparations. As an example, note Figs. 6 and 7, corresponding to the original ondansetron hydrochloride and to ondansetron hydrochloride dissolved in methanol, respectively, and in which irregular shapes with no fixed form can be observed. There seems to be no differences between the crystalline forms of the two, as expected after observing the powder X-ray diffraction diagrams.

In view of the results of this study, we conclude that the PXRD data demonstrate that there is

no crystallographic polymorphism in ondansetron hydrochloride, which is confirmed by the microphotographs. Rather, physical structural changes may have taken place, which would be of interest from the pharmaceutical point of view.

Ondansetron hydrochloride is a stable molecule and remains unaffected by the organic solvents used or by the temperatures to which it was subjected.

## REFERENCES

1. Gennaro, A.R.; et al., Eds. *Remington Farmacia*, 19th Ed.; Médica Anamericana: Buenos Aires, Argentina, 1995; 2226.
2. Helman, J. *Pharmacotecnia Teórica y Práctica*; Continental: Mexico D.F., 1980; 1139–1143.
3. Lácer, J.M.; Gallardo, V.; Parera, A.; Ruiz, M.A. Formation of Ondansetron Polymorphs. *Int. J. Pharm.* **1999**, *177*, 221–229.
4. Blackwell, C.P.; Harding, S.M. The Clinical Pharmacology of Ondansetron. *Eur. J. Cancer Clin. Oncol.* **1989**, *25* (suppl. 1), 21–24.
5. Freeman, A.J.; et al. Selectivity of 5-HT<sub>3</sub> Receptor Antagonist and Anti-emetic Mechanisms of Action. *Anti-cancer Drugs* **1991**, *3*, 79–85.
6. Roita, F.; Del Favero, A. Ondansetron Clinical Pharmacokinetics. *Clin. Pharmacokinetics* **1995**, *29* (2), 94–108.
7. Sheldrick, G.M. *SHELXTL-Plus. Program for the Solution of Crystal Structures*, Release 3.4; University of Göttingen: Göttingen, Germany, 1989.
8. Hughes, J.C.; Brown, G. J. *Soil Sci.* **1971**, *30*, 557–563.



Copyright of Drug Development & Industrial Pharmacy is the property of Taylor & Francis Ltd and its content may not be copied or emailed to multiple sites or posted to a listserv without the copyright holder's express written permission. However, users may print, download, or email articles for individual use.